The Plant Cell, Vol. 18, 2650–2663, October 2006, www.plantcell.org © 2006 American Society of Plant Biologists

A Pentatricopeptide Repeat Protein Facilitates the *trans*-Splicing of the Maize Chloroplast *rps12* Pre-mRNA [W]

Christian Schmitz-Linneweber,[1] Rosalind E. Williams-Carrier, Pascale M. Williams-Voelker, Tiffany S. Kroeger, Athea Vichas,[2] and Alice Barkan[3]

Institute of Molecular Biology, University of Oregon, Eugene, Oregon 97403

The pentatricopeptide repeat (PPR) is a degenerate 35–amino acid repeat motif that is widely distributed among eukaryotes. Genetic, biochemical, and bioinformatic data suggest that many PPR proteins influence specific posttranscriptional steps in mitochondrial or chloroplast gene expression and that they may typically bind RNA. However, biological functions have been determined for only a few PPR proteins, and with few exceptions, substrate RNAs are unknown. To gain insight into the functions and substrates of the PPR protein family, we characterized the maize (*Zea mays*) nuclear gene *ppr4*, which encodes a chloroplast-targeted protein harboring both a PPR tract and an RNA recognition motif. Microarray analysis of RNA that coimmunoprecipitates with PPR4 showed that PPR4 is associated in vivo with the first intron of the plastid *rps12* pre-mRNA, a group II intron that is transcribed in segments and spliced in trans. *ppr4* mutants were recovered through a reverse-genetic screen and shown to be defective for *rps12 trans*-splicing. The observations that PPR4 is associated in vivo with *rps12-intron 1* and that it is also required for its splicing demonstrate that PPR4 is an *rps12 trans*-splicing factor. These findings add *trans*-splicing to the list of RNA-related functions associated with PPR proteins and suggest that plastid group II *trans*-splicing is performed by different machineries in vascular plants and algae.

INTRODUCTION

Chloroplasts and mitochondria evolved from free-living bacteria and retain remnants of their ancestral bacterial genomes. The organellar genomes encode essential components of the photosynthetic and respiratory machineries, and the expression and regulation of these genes require the participation of nuclear gene products. Surprises to emerge from recent research in this area include the large number of nuclear genes involved and the recognition that many nuclear genes that modulate organellar gene expression were not derived from the bacterial ancestor but instead were co-opted from the nuclear genome during a process of nuclear-organellar coevolution (Dyall et al., 2004; Gray, 2004). These principles are highlighted by a recently recognized protein family that is largely specific to plants, the pentatricopeptide repeat (PPR) family. The PPR family is characterized by tandem repeats of a degenerate 35–amino acid motif that is related to the tetratricopeptide repeat motif (Small and Peeters, 2000). Several PPR proteins are encoded in animal and fungal genomes, and ~20 PPR proteins are encoded in trypanosome genomes (Mingler et al., 2006), but the family is greatly expanded in seed plants, with >400 hundred members in *Arabidopsis thaliana* and rice (*Oryza sativa*; Lurin et al., 2004). Most of these proteins are predicted to be targeted to chloroplasts or mitochondria, and all but one of the ~15 PPR proteins that have been genetically characterized affect the processing or translation of specific organellar RNAs (Barkan et al., 1994; Manthey and McEwen, 1995; Coffin et al., 1997; Fisk et al., 1999; Ikeda and Gray, 1999; Lown et al., 2001; Mancebo et al., 2001; Auchincloss et al., 2002; Bentolila et al., 2002; Desloire et al., 2003; Hashimoto et al., 2003; Kazama and Toriyama, 2003; Koizuka et al., 2003; Meierhoff et al., 2003; Mili and Pinol-Roma, 2003; Williams and Barkan, 2003; Xu et al., 2004; Yamazaki et al., 2004; Kotera et al., 2005; Prasad et al., 2005; Mingler et al., 2006; Wang et al., 2006); the lone exception, *Arabidopsis* GRP23, is a nuclear protein that is proposed to regulate transcription (Ding et al., 2006). By extrapolation, it is anticipated that the PPR family plays a central and broad role in modulating gene expression in both mitochondria and chloroplasts.

The consistent genetic data implicating PPR proteins in RNA-related functions, the observation that several PPR proteins bind nucleic acids in vitro (Ikeda and Gray, 1999; Lahmy et al., 2000; Mancebo et al., 2001; Nakamura et al., 2003; Lurin et al., 2004), and structural modeling of PPR tracts based on established structures for tetratricopeptide repeat tracts (Small and Peeters, 2000; Williams and Barkan, 2003) together suggest that PPR proteins typically bind directly to specific organellar RNA sequences through a surface created by stacked helical repeating units. However, there are little data that link phenotypes of PPR mutants to specific RNA targets or that address mechanisms by which PPR proteins bind RNA and influence downstream processes. The identification of the specific in vivo ligands of PPR proteins is

[1] Current address: Molekulare Genetik, Institut für Biologie, Humboldt-Universität, Berlin, Germany.
[2] Current address: Department of Molecular Biology, Weill Graduate School of Medical Sciences, Cornell University, New York, NY, 10021.
[3] To whom correspondence should be addressed. E-mail abarkan@molbio.uoregon.edu; fax 541-346-5891.
The authors responsible for distribution of materials integral to the findings presented in this article in accordance with the policy described in the Instructions for Authors (www.plantcell.org) are: Christian Schmitz-Linneweber (christian.schmitz-linneweber@rz.hu-berlin.de) and Alice Barkan (abarkan@molbio.uoregon.edu).
[W] Online version contains Web-only data.
www.plantcell.org/cgi/doi/10.1105/tpc.106.046110

a prerequisite for addressing these issues. Recently, we used a technique termed RIP-chip (for RNA coimmunoprecipitation and chip hybridization) to pinpoint the in vivo RNA ligands of the maize (*Zea mays*) PPR protein CRP1 (Schmitz-Linneweber et al., 2005). In a RIP-chip experiment, RNAs that coimmunoprecipitate with specific proteins from chloroplast extract are identified by hybridization to a plastid genome tiling microarray. RIP-chip data showed that CRP1 is associated in vivo with the 5′ untranslated regions of the *psaC* and *petA* mRNAs (Schmitz-Linneweber et al., 2005), the two plastid mRNAs whose translation CRP1 activates (Barkan et al., 1994). This study revealed a consensus sequence shared by the two RNA segments with which CRP1 is associated. However, analogous information for more PPR proteins will be needed before general themes that underlie PPR–RNA interactions will emerge.

Here, we analyzed the functions and RNA ligands of another maize chloroplast PPR protein, which we named PPR4. PPR4 (and its orthologs) is the only predicted plant protein to have both a PPR tract and an RNA recognition motif (RRM) RNA binding domain. Exploring the contribution of these two RNA binding domains to recognition and metabolism of target transcripts may help to delineate the functions of these two common RNA binding domains in higher plants. We show here that PPR4 is required for the accumulation of the *trans*-spliced chloroplast *rps12* mRNA and consequently for the accumulation of plastid ribosomes. We show further that PPR4 is associated with *rps12* intron RNA in vivo, indicating that PPR4 functions directly, rather than indirectly, in *rps12* intron metabolism. These results add group II intron *trans*-splicing to the repertoire of RNA-related functions described for PPR proteins. In addition, these findings add another layer to the emerging understanding of protein-facilitated group II intron splicing: PPR4 is the only protein that functions specifically in *trans*-splicing to be described in land plants, and it is unrelated to the three group II *trans*-splicing factors identified in *Chlamydomonas reinhardtii* chloroplasts (Perron et al., 1999; Rivier et al., 2001; Merendino et al., 2006), to the four group II *cis*-splicing factors previously identified in maize chloroplasts (Jenkins and Barkan, 2001; Till et al., 2001; Ostheimer et al., 2003), or to known proteins that facilitate the splicing of group II introns in bacteria and fungal mitochondria (Carignani et al., 1983, 1986; Lambowitz and Perlman, 1990; Huang et al., 2005; Mohr et al., 2006). These results support the view that the highly dissimilar intron sets of streptophyte and chlorophyte chloroplasts are served by independently acquired sets of splicing factors.

RESULTS

PPR4 Is the Only Predicted Plant Protein with Both a PPR and an RRM Domain

The PlantRBP database (http://plantrbp.uoregon.edu/) provides a tool to search for orthologous proteins in rice and *Arabidopsis* with specified domain content and predicted intracellular location. A search for proteins that are predicted to be chloroplast targeted and to have both an RRM and a PPR domain returned one *Arabidopsis* protein, At5g04810, which was assigned to an orthologous group with rice Os04g58780. Orthology between At5g04810 and Os04g58780 is supported by the facts that they are mutual best hits in whole-proteome BLAST comparisons between rice and *Arabidopsis*, that they cluster in a phylogram that includes the most closely related rice and *Arabidopsis* proteins (see http://plantrbp.uoregon.edu/), and that their intron number and position are conserved. BLASTN queries of public maize sequence data with the nucleotide sequence of Os04g58780 detected a putative maize ortholog that also encodes a PPR tract and an RRM domain; this sequence detects the initial query, Os0458780, as its top hit in BLASTN searches of the rice genome, supporting their orthology. No evidence for other closely related paralogs exists among available maize sequence data. We named this maize gene *ppr4*.

A *ppr4* cDNA clone obtained from the *Z. mays* full-length cDNA collection (http://www.genome.arizona.edu/orders/) was sequenced in its entirety. The sequence, which includes the complete open reading frame, has been deposited in GenBank (accession number DQ508419). An alignment of maize PPR4 and its apparent rice and *Arabidopsis* orthologs is shown in Figure 1. All three proteins have a predicted chloroplast transit peptide at their N terminus, followed by an RRM domain and 16 tandem PPR motifs (Figure 1).

Recovery of Loss-of-Function *ppr4* Alleles

To determine the function of PPR4, we initiated a reverse-genetic approach in both *Arabidopsis* and maize. We obtained three T-DNA insertions in At5g04810 (At *PPR4*) from the ABRC (Alonso et al., 2003). The positions of the T-DNA inserts in all three lines were confirmed by PCR analysis and DNA sequencing (see Supplemental Figure 1 online). After self-pollination, seed from each of the three insertion lines was germinated on Murashige and Skoog medium, and >20 of the germinating progeny from each line were analyzed by PCR to detect the T-DNA insertion. Approximately two-thirds of the germinating plants were heterozygous for the expected insert in each line, but no homozygous mutant plants were detected. Furthermore, among ~250 seeds analyzed from plants heterozygous for each of the three insertions, ~25% were shriveled and aborted (data not shown). The fact that three independent insertions in At *PPR4* are genetically linked to an abortive-seed phenotype strongly suggests that this gene is essential for embryogenesis in *Arabidopsis*. Disruption of several other genes for chloroplast-targeted PPR proteins has also been reported to cause embryo lethality in *Arabidopsis* (Lurin et al., 2004; Cushing et al., 2005).

Maize *ppr4* mutants were obtained through a PCR-based screen of our collection of *Mu* transposon–induced nonphotosynthetic mutants (http://chloroplast.uoregon.edu/) (Stern et al., 2004) (see Methods). Two mutant alleles were recovered: the *ppr4-1* allele has a *Mu9* element in the protein-coding region, near the 3′ end of exon 1 (Figures 1 and 2A); and the *ppr4-2* allele has a *Mu1* element inserted in the first intron, 94 bp downstream of the 5′ splice junction (Figure 2A). In contrast with homozygous At *PPR4* mutants, the homozygous maize mutants germinated and gave rise to chlorophyll-deficient seedlings: *ppr4-1*/*ppr4-1* seedlings are albino, whereas *ppr4-2*/*ppr4-2* seedlings are slightly pale green (Figure 2B); both are seedling lethal at ~3 weeks after germination, as is typical of nonphotosynthetic maize mutants. Crosses between *ppr4-1*/+ and *ppr4-2*/+ plants yielded mutant plants of an intermediate phenotype (Figure 2B)

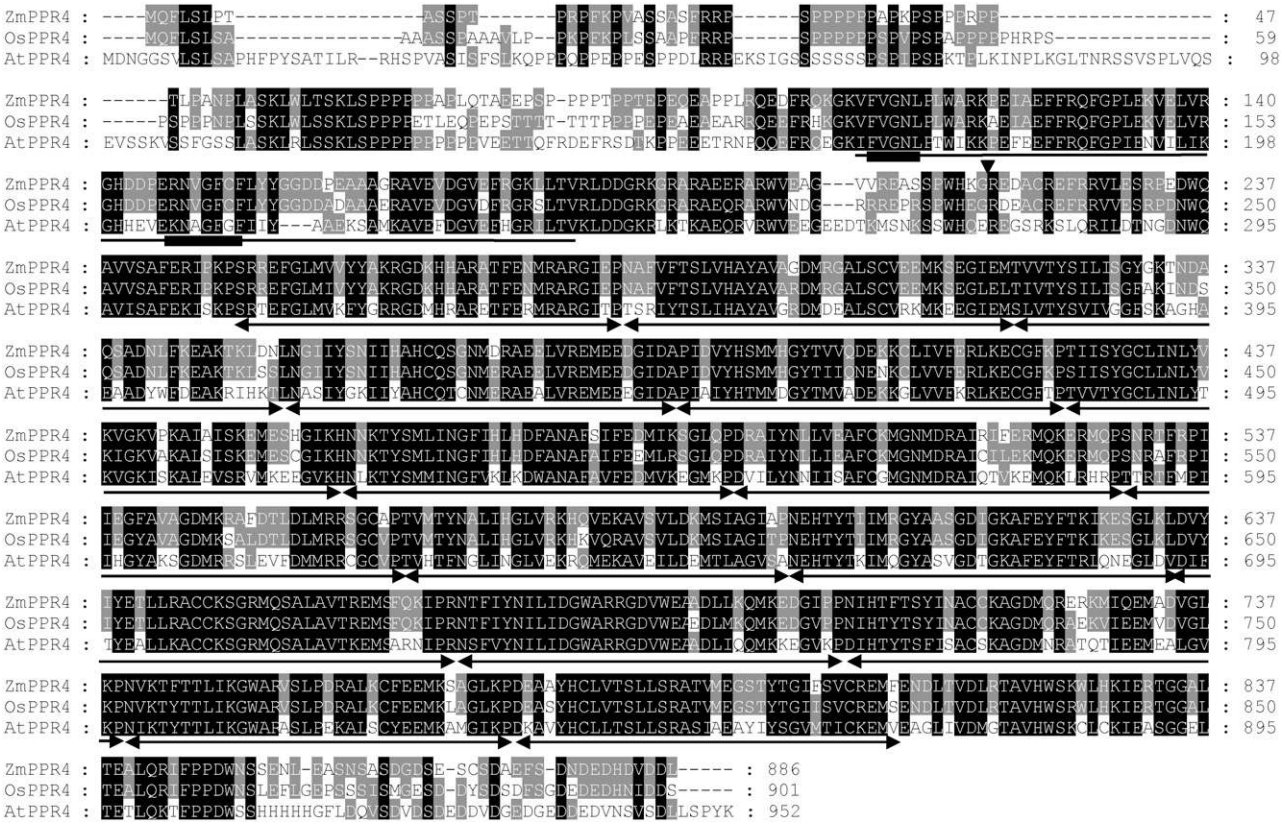

Figure 1. Alignment of PPR4 Orthologs in Maize (Zm), Rice (Os), and *Arabidopsis* (At).

TargetP (Emanuelsson et al., 2000) and Predotar (Small et al., 2004) algorithms both predict that all three proteins are targeted to the chloroplast. The insertion site of the *Mu9* element in *ppr4-1* mutants is indicated by an arrowhead. The RRM domain is underlined, with the thicker lines denoting its two core RNP motifs. PPR repeats are indicated below the sequences by double-headed arrows. At PPR4 corresponds to Arabidopsis Genome Initiative locus At5g04810; Os PPR4 corresponds to The Institute for Genomic Research locus Os04g58780.

at the expected 1:3 ratio of mutant-to-normal plants, confirming that the chlorophyll-deficient phenotypes are due to the insertions in the *ppr4* gene. Chloroplasts could be isolated from *ppr4-1/ppr4-2* plants but not from the albino *ppr4-1/ppr4-1* plants, so *ppr4-1/ppr4-2* material was used in experiments described below that required chloroplast isolation.

The accumulation of *ppr4* mRNA in *ppr4-1/ppr4-2* mutant leaf tissue was compared with that in normal siblings and in leaves from the mutant *hcf7*, which has a similar chlorophyll-deficient phenotype and a related chloroplast gene expression defect (see below). Primers were designed to the first and second exons, such that amplification products from spliced mRNA and from genomic DNA could be distinguished. As expected, the *Mu* insertions cause a substantial reduction in the level of *ppr4* mRNA (Figure 2C). Residual *ppr4* mRNA in *ppr4-1/ppr4-2* plants is consistent with the weak phenotype of the *ppr4-2* allele, which has a *Mu* insertion within an intron that could be spliced out of the pre-mRNA.

PPR4 Resides in the Chloroplast Stroma

Antibody was raised to a recombinant PPR4 fragment and used to probe immunoblots of total leaf extract and subcellular fractions. A protein of the expected size (~100 kD) was strongly enriched in chloroplast extract, with respect to its concentration in total leaf extract where it was barely detectable (Figure 3A). Analysis of chloroplast subfractions showed that this protein localizes to the stromal fraction (Figure 3A). The abundance of this protein was strongly reduced in stroma from *ppr4-1/ppr4-2* mutant chloroplasts (Figure 3B), confirming that it is PPR4. These results show that PPR4 resides in the chloroplast stroma.

To determine whether PPR4 is stably bound to other macromolecules in vivo, chloroplast stroma was fractionated in sucrose gradients, and the distribution of PPR4 in the gradient was determined by immunoblotting (Figure 4, top panel). PPR4 was found primarily in fractions near the top of the gradient; this peak may represent monomeric PPR4. A small fraction of PPR4 was found in high molecular weight complexes that are larger than ribulose-1,5-bis-phosphate carboxylase/oxygenase (Rubisco) (marked with a bar in Figure 4), and some PPR4 was recovered in pelleted material at the bottom of the gradient (last lane). Treatment of stroma with RNase A prior to sedimentation reduced the recovery of PPR4 in the high molecular weight fractions but did not shift its position in the upper fractions (Figure 4, bottom panel). These results indicate that PPR4 is found

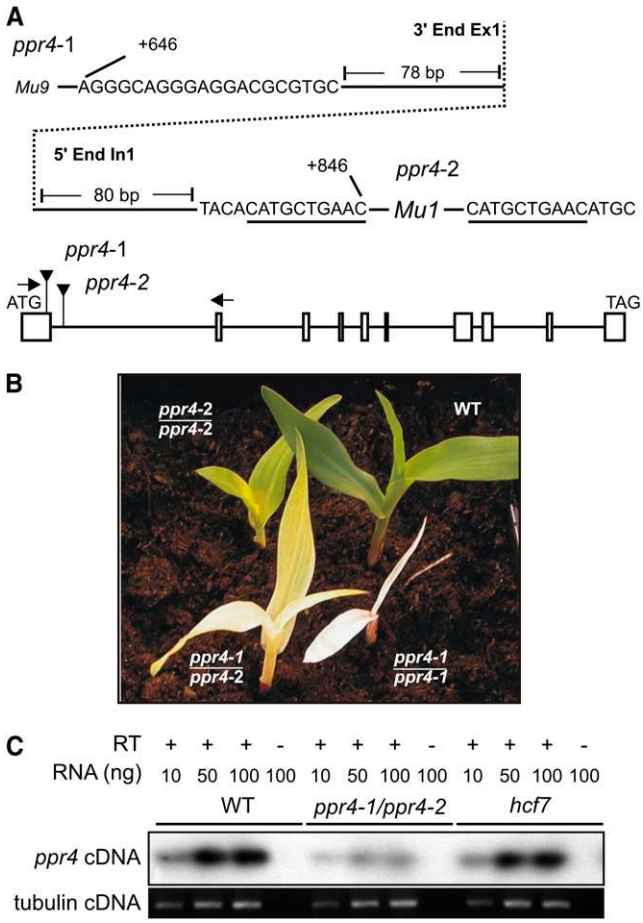

Figure 2. *Mu*-Induced *ppr4* Mutants.

(A) Positions of the *Mu* insertions in *ppr4-1* and *ppr4-2*. The DNA sequence flanking the *Mu* insertions is shown, with the intron-exon border indicated by a dotted line. Residue numbers with respect to the start codon in the genomic sequence are indicated. A 10-nucleotide duplication flanking the *ppr4-2* insertion site is underlined; this sequence is present only once in the progenitor allele. The type of *Mu* element at each site (i.e., *Mu1* or *Mu9*) was deduced from polymorphisms in the terminal inverted repeat sequences. A schematic representation of the *ppr4* gene is shown below. Boxes represent exons, and lines represent introns (drawn to scale). *Mu* element insertion sites are marked. Arrows illustrate the primers used for RT-PCR analysis of *ppr4* mRNA shown in **(C)**.

(B) Phenotypes of *ppr4* mutant seedlings. Plants were grown for 2 weeks in soil in a greenhouse.

(C) Decreased abundance of *ppr4* mRNA in *ppr4* mutants. *ppr4* mRNA was assayed by RT-PCR using primers in exons 1 and 2 (primer binding sites are diagrammed in **[A]**). Conditions were chosen to yield a signal that is roughly proportional to the amount of input RNA. RNA from an *hcf7* mutant, whose phenotype resembles that of *ppr4-1/ppr4-2* mutants (see Results), was analyzed to address the possibility that *ppr4* expression might be regulated in response to the status of plastid development/physiology. The bottom panel shows RT-PCR amplification of tubulin mRNA in the same RNA samples.

predominantly in small complexes or as a monomer and that a subpopulation is associated with high molecular weight complexes that include RNA.

PPR4 Is Required for the Accumulation of Plastid Ribosomes

The *ppr4-1* allele conditions an ivory leaf pigmentation similar to that seen in previously described mutants that lack plastid ribosomes (e.g., *ppr2*, *crs2-1*, and *iojap*) (Walbot and Coe, 1979; Jenkins et al., 1997; Williams and Barkan, 2003), suggesting that *ppr4* mutants might have plastid ribosome defects. In fact, RNA gel blots of leaf RNA from both ivory *ppr4-1/ppr4-1* and pale green *ppr4-2/ppr4-1* mutants revealed defects in plastid rRNAs (Figure 5A). Mature plastid 23S and 16S rRNAs were undetectable in *ppr4-1/ppr4-1* mutants, as in *ppr2*, *iojap*, and *crs2-1* mutants (Williams and Barkan, 2003). Mature plastid rRNAs are also reduced in pale green *ppr4-2/ppr4-1* mutants, albeit to a lesser extent. Interestingly, these mutants accumulate increased levels of a putative precursor to 16S rRNA (Figure 5A), a phenotype similar to that described previously for maize *hcf7* mutants (Barkan, 1993); 16S rRNA from *hcf7* is shown in Figure 5A for comparison. Accumulation of 16S rRNA precursors in bacteria is indicative of defective assembly of the small ribosomal subunit (Dahlberg et al., 1978; Srivastava and Schlessinger, 1989; Srivastava and Schlessinger, 1990). These results suggested

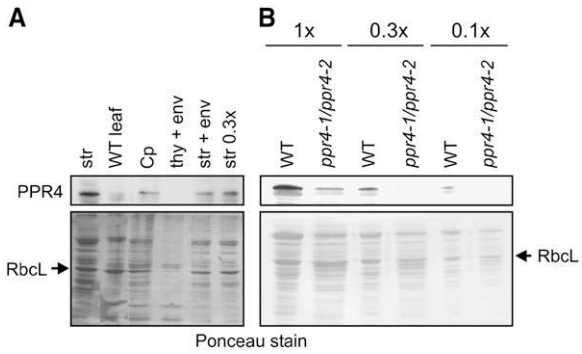

Figure 3. PPR4 Resides in the Chloroplast Stroma.

Immunoblots were probed with affinity-purified anti-PPR4 antibody. The bottom panels show the same blots stained with Ponceau S prior to probing. RbcL, large subunit of Rubisco.

(A) Immunoblot of leaf and subcellular fractions. The total chloroplast fraction (Cp) and the thylakoid+envelope (thy+env) and stroma+envelope (str+env) subfractions were from the fractionated chloroplast preparation described and verified with marker proteins by Williams and Barkan (2003) and are derived from the same quantity of starting chloroplasts. The stromal fraction (str) and its dilution (str 0.3x) are from a separate preparation.

(B) Verification that the 100-kD protein detected by the PPR4 antibody is PPR4. An equal quantity of stromal protein from wild-type and *ppr4-1/ppr4-2* chloroplasts (1x) or dilutions thereof (0.3x and 0.1x) were analyzed. The *ppr4* mutant material is from a complementation cross between a null and weak allele and retains some *ppr4* expression. Antisera from two different rabbits yielded similar results (data not shown).

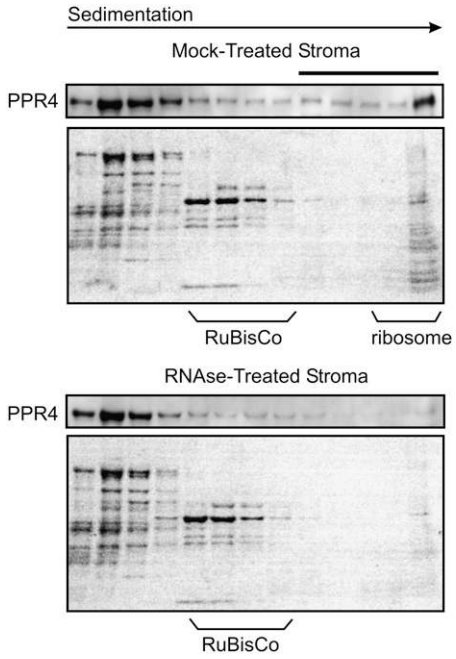

Figure 4. Sucrose Gradient Analysis of PPR4-Containing Particles in Stromal Extract.

Stromal extract was treated with RNase A (RNase-treated) or incubated under the same conditions in the absence of RNase (mock-treated) and sedimented through sucrose gradients. An equal volume of each gradient fraction was analyzed on immunoblots probed with PPR4 antibody. Images of the blots stained with Ponceau S are shown below to illustrate the similar fractionation of Rubisco and other abundant proteins in the two gradients. The last lane in each panel contains material that pelleted in the gradients. The position of ribosomes was determined by the pattern of Ponceau S–stained bands and by the appearance of rRNAs in these fractions (data not shown). A high molecular weight, RNase-sensitive peak of PPR4 is indicated with a solid bar.

that PPR4 functions in a process that is needed for the biogenesis of small ribosomal subunits in plastids.

As anticipated for plants with a plastid ribosome deficiency, *ppr4-2/ppr4-1* mutants accumulate reduced levels of all photosynthetic enzyme complexes that include plastid-encoded subunits (Rubisco, photosystem II, cytochrome b_6f, photosystem I, and ATP synthase) (Figure 5B). In the more severe *ppr4-1/ppr4-1* mutants, these proteins were not detectable (data not shown). Thus, *ppr4* mutants have a global defect in plastid gene expression.

PPR4 Is Associated in Vivo with the Group II Intron from the *trans*-Spliced Plastid *rps12* Pre-mRNA

Previously studied PPR proteins influence the processing or translation of specific organellar RNAs. Therefore, it seemed plausible that the plastid ribosome deficiency in *ppr4* mutants was due to an underlying defect in the expression of just one or several components of the plastid translation machinery. For example, a primary defect in the maturation of the 16S rRNA or of an mRNA encoding a protein in the small ribosomal subunit would be anticipated to result in the ribosome deficiency and aberrant 16S rRNA processing observed in *ppr4* mutants.

To gain insight into the direct target(s) of PPR4, we used the RIP-chip assay (Schmitz-Linneweber et al., 2005) to identify plastid RNAs that are associated with PPR4 in chloroplast extract. PPR4 was immunoprecipitated from stromal extract prepared from wild-type chloroplasts, and RNA purified from the immunoprecipitation pellet and supernatant was labeled with red- and green-fluorescing dyes, respectively. The pellet and supernatant RNAs were competitively hybridized to a chloroplast genome tiling microarray. The ratio of red to green fluorescence for each spot reflects the degree to which the corresponding RNA sequence is enriched in the immunoprecipitation pellet. As a negative control, immunoprecipitations were also performed with stromal extract from *ppr4-2/ppr4-1* mutant chloroplasts, which accumulate reduced levels of PPR4 protein (Figure 3B). The null *ppr4-1/ppr4-1* mutants could not be used for this purpose because we have been unable to obtain sufficient yields of stroma from albino plants for RIP-chip analysis. PPR4-associated RNAs were identified as RNAs that were significantly more enriched in immunoprecipitations from wild-type stroma than in immunoprecipitations from *ppr4* mutant stroma.

Two replicate experiments were performed with wild-type stroma and two with *ppr4-2/ppr4-1* mutant stroma. The replicate experiments were performed with antibodies from two different immunized rabbits. Data from the four assays were normalized and used to calculate median enrichment ratios (i.e., ratio of red

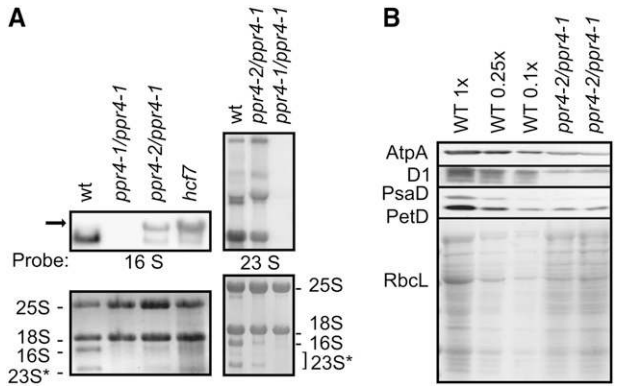

Figure 5. Loss of Plastid rRNAs and Plastid-Encoded Proteins in *ppr4* Mutants.

(A) RNA gel blot hybridizations showing plastid rRNA defects in *ppr4* mutants. Five micrograms of total leaf RNA was analyzed by hybridization to probes for the plastid 16S or 23S rRNA. The same filters stained with methylene blue are shown below: bands corresponding to cytosolic rRNAs (25S and 18S) and plastid rRNAs (16S and 23S*) are marked. 23S* is a breakdown product of the plastid 23S rRNA. The arrow indicates the 16S rRNA precursor that overaccumulates in *ppr4* and *hcf7* mutants.
(B) Immunoblot analysis of photosynthetic enzyme accumulation in *ppr4* mutants. Total leaf proteins of *ppr4-1/ppr4-2* mutants were analyzed by probing immunoblots with antisera to representative subunits of photosystem I (PsaD), photosystem II (D1), ATP synthase (AtpA), and the cytochrome b_6f complex (PetD). The same filter was stained with Ponceau S to visualize total proteins (bottom); the large subunit of Rubisco (RbcL) is indicated on the stained blot.

to green fluorescence) for each DNA fragment among the replicate spots (five per array) and replicate experiments (see Supplemental Tables 1 and 2 and Supplemental Figure 2 online). To visualize sequences that were preferentially enriched from the wild-type extract, the difference in median enrichment ratio for each DNA fragment between the wild-type and mutant experiments was plotted as a function of chromosomal position (Figure 6A). Two prominent peaks of differential enrichment were observed, both of which mapped to DNA fragments encoding the first intron in the *rps12* gene (*rps12-int1*). *rps12-int1* is a group II intron that is transcribed in two pieces from distinct chromosomal loci and then spliced in trans (Koller et al., 1987; Hildebrand et al., 1988) (see map in Figure 6D). Array elements from both loci stood out as red fluorescing spots when probed with immunoprecipitated RNA from wild-type stroma but not when probed with immunoprecipitated RNA from *ppr4* mutant stroma (Figure 6B; data not shown).

Table 1 summarizes the data for the DNA fragments whose enrichment from wild-type stroma ranked in the top 10% among the 248 fragments on the array; fragments in the table are ordered according to the degree to which they are differentially enriched from wild-type versus *ppr4* mutant extract. A *t* test was used to evaluate the null hypothesis that sequences corresponding to each fragment were enriched to the same extent from wild-type and *ppr4* mutant stroma. A P value below 3×10^{-4} indicates significant enrichment, as this cutoff would be anticipated to yield <0.1 false positives among the 248 distinct DNA fragments (each in five replicate spots) on the array. Coenrichment of adjacent fragments further increases confidence that the corresponding RNAs were enriched and was observed in both regions encoding *rps12-int1* (fragments 193 and 194 and fragments 128 to 131). Furthermore, all five fragments that include sequences from *rps12-int1* (fragments 130, 131, 132, 193, and 194) are among the top eight ranking fragments, and all five show highly significant preferential enrichment from wild-type extract (P values $<10^{-5}$) (Table 1). Many of the other high-ranking fragments are from sequences adjacent to *rps12-int1* (e.g., 129, 190, 195, and 196) and were presumably enriched due to their presence on the same RNA molecules as *rps12-int1.* Therefore, the RIP-chip data provide strong evidence that PPR4 interacts with *rps12* pre-mRNA in vivo, as exon 1, both fragments of intron 1, and exon 2 showed highly significant PPR4-dependent enrichment during PPR4 immunoprecipitations.

To verify the RIP-chip data and to further pinpoint the RNA sequences with which PPR4 is associated, RNAs that coimmunoprecipitate with PPR4 were analyzed by slot blot hybridization. As a control, parallel assays were performed with antibody to the chloroplast splicing factor CRS1, which is known to be associated specifically with the *atpF* intron in vivo (Till et al., 2001; Ostheimer et al., 2003). RNAs purified from the immunoprecipitation pellets and supernatants were applied through a slot blot manifold to nylon membrane. Duplicate slot blots were probed with radiolabeled PCR products representing different segments of the *rps12* gene (see Figure 6D for probe positions) or the *atpF* intron. All of the *rps12* sequences were strongly enriched by immunoprecipitation with PPR4 antibody but not by immunoprecipitation with CRS1 antibody (Figure 6C). Specificity of these results is further shown by the fact that *atpF* intron RNA coimmunoprecipitated with CRS1 but not with PPR4. Furthermore, the two *rps12-int1* fragments were markedly more enriched than the flanking exons in the PPR4 immunoprecipitation pellets (compare probes B and C to probes A and D), as suggested by the RIP-chip data. These results confirm that PPR4 is associated with *rps12* pre-mRNA sequences in chloroplast extract and further point to the *trans*-spliced intron 1 as harboring one or more site with which PPR4 is associated.

The RIP-chip data did not provide strong evidence for other PPR4 interaction sites (see Table 1) but also did not eliminate the possibility that PPR4 might be associated with additional sequences. For example, the second group II intron in *rps12* showed significant PPR4-dependent enrichment, albeit with an enrichment ratio ~16-fold lower than that for *rps12-int1* (see fragment 190 in Table 1); this modest enrichment could result from the fact that intron 2 will be coprecipitated with intron 1 due to its location on the same pre-mRNA molecule, or it could reflect a distinct PPR4 binding site. The data also hinted at the possibility that fragments 139 and 142 (*petB*), 169 (*rpl2*), 243/244 (*ndhA*), and 156 (*infA*) might be enriched in a PPR4-dependent fashion; these are among the top-ranking 20% of fragments in terms of their enrichment from wild-type extract and may be differentially enriched from wild-type versus *ppr4* mutant extract (P values <0.01). However, the phenotypic analyses of *ppr4* mutants described below suggest that these results do not reflect meaningful physiological interactions.

PPR4 Is Required for *rps12 trans*-Splicing

The association between PPR4 and the *trans*-spliced *rps12* intron suggested that PPR4 might function in *rps12 trans*-splicing. A defect of this nature could account for the plastid ribosome deficiency and aberrant 16S rRNA metabolism observed in *ppr4* mutants. We therefore analyzed the accumulation of *rps12* transcripts in *ppr4* mutants.

Mutants with severe plastid ribosome deficiencies are albino, lack all chloroplast-encoded proteins, and exhibit a variety of stereotypical defects in chloroplast RNA metabolism (Han et al., 1993, 1995; Hess et al., 1993; Jenkins et al., 1997; Williams and Barkan, 2003). As a consequence, it can be difficult to identify the underlying molecular lesion in albino mutants through analysis of plastid proteins and transcript patterns (for an example, see Williams and Barkan, 2003). The severe *ppr4-1/ppr4-1* mutants are albino and lack plastid rRNAs (Figures 2B and 5A) and so were anticipated to share the stereotypical plastid transcript profiles with other mutants of this type. To reduce these pleiotropic effects, we analyzed RNA from the *ppr4-1/ppr4-2* progeny of complementation crosses, as these accumulate some chlorophyll, plastid rRNAs, and chloroplast-encoded proteins (Figures 2B and 5), albeit to reduced levels. To control for effects resulting from aberrant assembly of 30S ribosomal subunits, RNA from *hcf7* mutants was analyzed in parallel; *hcf7* mutants resemble *ppr4-1/ppr4-2* mutants in having a global plastid translation defect, aberrant 16S rRNA processing, and decreased chlorophyll content (Barkan, 1993).

RNAs from the wild type, *ppr4-1/ppr4-2* mutants, and *hcf7* mutants were analyzed by RNA gel blot hybridization using a series of probes derived from the *rps12* gene (Figure 7). The

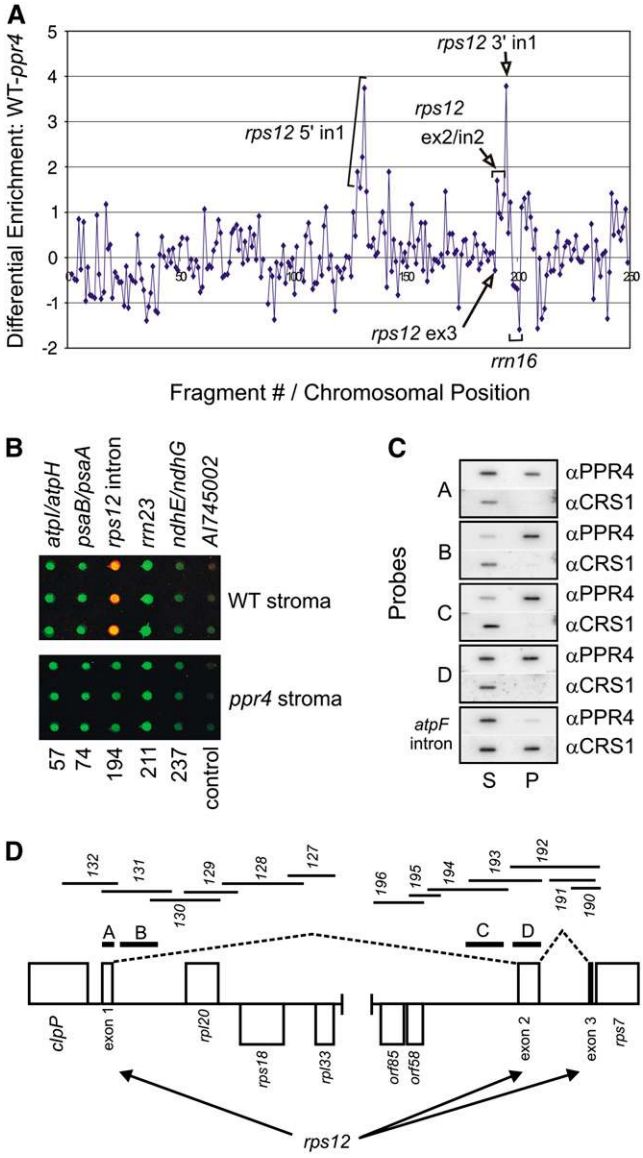

Figure 6. Identification of RNAs Associated with PPR4 in Chloroplast Stroma.

(A) Summary of RIP-chip data. The $\log_2$-transformed enrichment ratios (F635:F532) were normalized between two assays involving wild-type stroma and two control assays with *ppr4-1/ppr4-2* mutant stroma. The median normalized values for replicate spots from the mutant data were subtracted from those from wild-type data and plotted according to fragment number. Fragments are numbered according to chromosomal position. The data used to generate this figure are provided in Supplemental Tables 1 and 2 online and have been submitted to MIAME Express (accession number E-MEXP-716). The data from each of the four assays are plotted separately in Supplemental Figure 2 online to illustrate the reproducibility of the results.

(B) Excerpts of merged fluorescent images from representative PPR4 RIP-chip experiments involving wild-type and *ppr4-1/ppr4-2* mutant stroma. Fragment names are indicated above, and fragment numbers are indicated below. Each DNA fragment is represented five times on the array in clusters of two and three spots. These excerpts show three-spot clusters. AI745002 is a cytosolic cDNA used as a negative control.

smallest transcript detected with both exon 1 and exon 2 probes (probes A and D, ~1200 nucleotides) was strongly reduced in *ppr4* mutants but not in *hcf7* mutants (arrows in Figure 7). This transcript was not detected with the intron probes and thus represents a *trans*-spliced product of the two precursor RNAs. In addition, a putative unspliced precursor (a transcript of ~2500 nucleotides that hybridized to probes C and D) accumulated to increased levels in *ppr4* mutants (asterisk in Figure 7), although this transcript may be at increased levels in the *hcf7* mutant as well. Together, these results suggest that *rps12 trans*-splicing is disrupted in *ppr4* mutants, as the mutants accumulate reduced levels of the spliced 1200-nucleotide RNA and increased levels of a putative unspliced precursor.

To more clearly assess splicing of *rps12-int1* in *ppr4* mutants, the ratio of spliced versus unspliced RNA was quantified with a poisoned primer extension assay. In this assay, a radiolabeled oligonucleotide complementary to the second exon of *rps12* was used to prime a reverse transcription reaction in the presence of a dideoxy nucleotide that terminates after different distances on spliced and unspliced RNA templates (see diagram in Figure 8). With this assay, all transcripts in which *rps12-int1* is spliced are detected as one band, and all those in which this intron is retained are detected as a second band. As suggested by the RNA gel blot hybridizations, this assay showed that the vast majority of *rps12* transcripts in *ppr4-1/ppr4-2* mutants retain *rps12-int1*, whereas the ratio of spliced to unspliced RNA is unaltered in *hcf7* mutants (Figure 8). These results indicate that PPR4 functions either in the *trans*-splicing of *rps12-int1* or in stabilizing the spliced RNA. A role in *trans*-splicing rather than mRNA stabilization is supported by the increased accumulation of an unspliced precursor in *ppr4* mutants (Figure 7) and by the coimmunoprecipitation data suggesting that PPR4 is associated with intron sequences rather than exon sequences.

Several previously identified chloroplast group II intron splicing factors are associated with and required for the splicing of multiple introns (Jenkins et al., 1997; Ostheimer et al., 2003). Although the RIP-chip data for PPR4 did not provide strong evidence for its association with introns other than *rps12-int1*, they suggested the possibility of a weak association with *rps12-int2*, with the intron-containing *petB*, *rpl2*, and *ndhA* RNAs, and with the intronless *infA* and *rps18* RNAs. To address whether PPR4 influences the metabolism of these RNAs, their processing was assayed by RNA gel blot hybridization and poisoned primer extension (see Supplemental Figure 3 online). Minor changes in the transcript populations from some of these genes were observed, but these changes were similar to those in *hcf7* mutants

(C) Slot blot hybridizations to verify the coimmunoprecipitation of *rps12* RNAs with PPR4. One-third of the RNA recovered from each immunoprecipitation pellet (P) and one-sixth of the RNA recovered from each supernatant (S) were applied to replicate slot blots and hybridized with probes A through D (see **[D]**) or to *atpF* intron DNA. An immunoprecipitation with antibody to the *atpF* splicing factor CRS1 was used as a negative control.

(D) Schematic map of the split *rps12* gene and its flanking genes (not drawn to scale). Probes used for slot blot hybridizations are indicated with thick bars and are labeled with letters. DNA fragments on the array are indicated with thin bars and are labeled with their fragment number.

Table 1. Top-Ranking Fragments in PPR4 RIP-Chip Assays

Fragment Name	Fragment Number[a]	Wild-Type Stroma Median Log_2 Ratio (E)[b]	Wild-Type Stroma n[b]	*ppr4* Mutant Stroma Median Log_2 Ratio (E)[b]	*ppr4* Mutant Stroma n[b]	Comparison: Wild-Type versus *ppr4* Stroma Differential Enrichment ($E_{WT} - E_{ppr4}$)	Comparison: Wild-Type versus *ppr4* Stroma P Value[c]
rps12int13′	**194**	**2.51**	**10**	**−1.28**	**10**	**3.79**	**4.93E-15**
rps12int15′ex1	**131**	**2.05**	**9**	**−1.69**	**10**	**3.74**	**9.98E-09**
rpl20/rps12int15′	**130**	**0.36**	**9**	**−1.86**	**10**	**2.21**	**3.28E-08**
rps18	**128**	**−1.20**	**10**	**−3.09**	**10**	**1.89**	**5.61E-06**
rps12int2A	**190**	**−1.98**	**9**	**−3.68**	**10**	**1.70**	**1.95E-06**
rps18/rpl20	**129**	**−0.77**	**10**	**−2.32**	**9**	**1.55**	**8.66E-09**
rps12ex1/clpP	**132**	**−0.84**	**9**	**−2.31**	**8**	**1.47**	**7.62E-06**
rps12ex2int13′	**193**	**−0.99**	**10**	**−2.39**	**10**	**1.40**	**4.06E-06**
orf58/orf85	**196**	**−1.26**	**10**	**−2.48**	**10**	**1.22**	**1.08E-03**
ndhAint	243	−2.15	10	−3.37	10	1.21	5.85E-02
psbH/petB5′	139	−1.91	9	−2.91	10	1.00	4.90E-02
infA	156	−1.55	10	−2.32	9	0.76	4.20E-03
ndhAintex1	244	−2.09	10	−2.66	7	0.56	3.57E-02
orf58	**195**	**−1.46**	**10**	**−2.01**	**10**	**0.55**	**6.04E-02**
orf173-3′	180	−1.36	10	−1.89	9	0.53	3.95E-02
rpl33	127	−1.65	10	−2.14	9	0.49	1.72E-03
orf139	176	−1.72	9	−2.12	10	0.39	1.91E-01
trnL-CAA	181	−1.92	10	−2.21	9	0.29	1.52E-01
rps2B	54	−1.62	8	−1.58	10	−0.04	2.51E-01
trnV-UACex2int	97	−2.02	9	−1.91	9	−0.11	5.18E-01
petN3prime	37	−1.77	8	−1.56	9	−0.21	8.15E-01
ycf9	20	−1.72	9	−1.40	10	−0.32	2.26E-02
psaC/ndhE/ndhG	236	−2.05	8	−1.65	7	−0.41	1.89E-01
rrn16-3prime	200	−0.68	6	0.92	6	−1.60	1.25E-01

Elements ranking in the top 10% for median normalized enrichment ratio (E) from wild-type stroma are ordered according to the magnitude of their differential enrichment from wild-type versus *ppr4* mutant stroma ($E_{WT} - E_{ppr4}$). Fragments that map within or adjacent to the two *rps12* loci are in boldface.

[a] Fragments on the array are numbered according to chromosomal position. The nucleotide residues on each fragment are described in Array Express (accession number A-MEXP-164) and in Supplemental Table 1 from Schmitz-Linneweber et al. (2005).

[b] E = median (log_2F635/F532) normalized across two replicate experiments with wild-type stroma and two with *ppr4-1/ppr4-2* mutant stroma. Replicate experiments constitute a total of *n* replicate spots with signal above background.

[c] P values were calculated with a *t* test (two-tailed, unequal variance) and represent the probability that there is no difference in enrichment from wild-type and mutant extract.

and so could be secondary effects of the ribosome deficiency. Therefore, the RIP-chip data together with the *ppr4* mutant phenotype suggest that PPR4 functions specifically in the *trans*-splicing of the *rps12* pre-mRNA and that this single function underlies the plastid ribosome deficiency and 16S rRNA processing defect in *ppr4* mutants.

DISCUSSION

Current data suggest that PPR proteins play a central and broad role in modulating the expression of organellar genes in plants. Although only a small fraction of PPR proteins have been studied, extrapolation from the available genetic and biochemical data leads to the prediction that most PPR proteins mediate specific posttranscriptional steps in organellar gene expression and that they do so via direct interaction with RNA. Despite their key role as integrators of nuclear and organellar functions, very little is known about the functions, substrates, or biochemical mechanisms of PPR proteins.

In this study, we have assigned a function and RNA substrate to a new member of the PPR family, maize PPR4. PPR4 and its orthologs in rice and *Arabidopsis* has 16 PPR motifs and an N-terminal RRM domain. We have shown that PPR4 is localized to the chloroplast stroma, where it is associated specifically with the first intron of the *rps12* pre-mRNA. This intron is transcribed in two pieces and spliced in trans. PPR4 is associated with both intron fragments in chloroplast extract, and it is required for the accumulation of the *trans*-spliced *rps12* mRNA in vivo. These results provide strong evidence that PPR4 is required for the *rps12 trans*-splicing reaction.

PPR Proteins as Group II Intron Splicing Factors

Group II introns are large ribozymes that are defined by a conserved predicted secondary structure consisting of six helical domains, characteristic interdomain interactions, and small regions of conserved primary sequence (Michel et al., 1989; Michel and Ferat, 1995). Some group II introns, including *rps12-int1*,

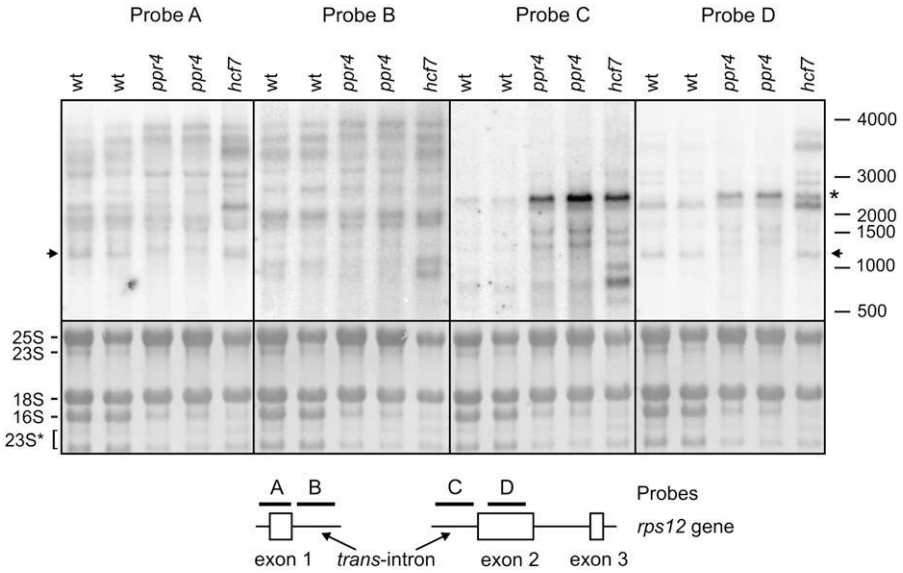

Figure 7. RNA Gel Blot Hybridizations of *rps12* Transcripts in *ppr4* Mutants.

Top panel: Total leaf RNA (5 μg/lane) was fractionated on a single agarose gel and transferred to a nylon membrane. The membrane was cut into four strips, which were hybridized with the indicated probes. Two different *ppr4* mutant seedlings (genotype *ppr4-1/ppr4-2)* and two different normal siblings (wt) were analyzed to provide replicate results. Transcripts that are missing in *ppr4* mutants are marked with an arrow. A transcript that accumulates to higher levels in *ppr4* mutants than in *hcf7* mutants is marked with an asterisk. Middle panel: rRNAs on the same filters were detected by staining with methylene blue. Bottom panel: Schematic of the *rps12* gene and probes used for the RNA gel blots.

have become fragmented during the course of evolution, such that they are transcribed in several pieces. During *trans*-splicing, the intron fragments assemble via noncovalent interactions and then splice out of the precursor RNA. *trans*-splicing has been described for several introns of plant mitochondria and algal chloroplasts (reviewed in Barkan, 2004), but in angiosperm chloroplasts, it is restricted to the *rps12* gene.

Both *cis*- and *trans*-spliced group II introns require protein cofactors to splice efficiently in vivo. These proteins fall into two general classes: conserved maturase proteins that are encoded within some group II introns, and diverse host-encoded proteins that were recruited from the host genomes. Three host-encoded protein complexes have been described that assemble with different subsets of the *cis*-spliced group II introns in maize chloroplasts and that facilitate their splicing in vivo (Jenkins et al., 1997; Jenkins and Barkan, 2001; Till et al., 2001; Ostheimer et al., 2003). Each of these complexes contains a member of a plant-specific protein family harboring a novel RNA binding domain called the CRM domain. The *Arabidopsis* PPR protein HCF152 is the only PPR protein previously suggested to function in group II intron splicing, as spliced chloroplast *petB* mRNA fails to accumulate in *hcf152* mutants (Meierhoff et al., 2003). However, excised *petB* intron accumulates normally in *hcf152* mutants, suggesting that HCF152 may function not in splicing but in the stabilization of the spliced *petB* mRNA.

It seems likely that the complement of proteins involved in group II *trans*-splicing is more complex than that involved in *cis*-splicing, as additional proteins may be required to assemble intron fragments. In fact, genetic studies indicate that at least 14 nuclear loci are required for the removal of the two *trans*-spliced introns in the *psaA* gene in *Chlamydomonas* chloroplasts (Goldschmidt-Clermont et al., 1990). Three of these genes have been cloned (Goldschmidt-Clermont et al., 1990; Rivier et al., 2001; Merendino et al., 2006); these proteins are not closely related to proteins in vascular plants, but one of them, Raa1, includes 38 amino acid repeats that resemble the 35–amino acid repeats of the canonical PPR motif (Merendino et al., 2006).

Data presented here show that PPR4 is required for the accumulation of the *trans*-spliced *rps12* intron in maize chloroplasts and that it is associated with the *rps12* intron RNA in vivo. These results, together with the fact that other RRM and PPR domains have been shown to bind RNA, strongly suggest that PPR4 facilitates *rps12 trans*-splicing through direct interaction with the intron RNA. It is noteworthy that a maturase protein is encoded by the *trans*-spliced *rps12* intron in the ancient charophytes *Staurastrum* and *Chaetosphoridium* (Turmel et al., 2002, 2005). Charophytes are among the closest algal sister groups of mosses, hornworts, liverworts, and vascular plants, where this maturase open reading frame was lost. It seems plausible that PPR4 might have replaced the ancient maturase proteins in *rps12 trans*-splicing.

Previously, we showed that the CAF2/CRS2 complex is required for *rps12 trans*-splicing and that it coimmunoprecipitates with *rps12* intron RNA (Ostheimer et al., 2003). Unlike PPR4, however, CAF2/CRS2 also facilitates the *cis*-splicing of several chloroplast group II introns. Thus, PPR4 may function in a process that is specific for *trans*-splicing (e.g., assembling the intron fragments or stabilizing their association), with CAF2/CRS2 promoting the subsequent splicing reaction. We have performed coimmunoprecipitation experiments to assess whether CAF2/

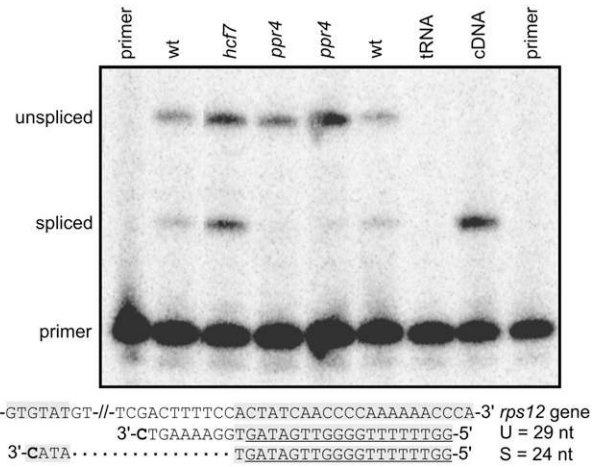

Figure 8. Poisoned Primer Extension Analysis Demonstrating Loss of *trans*-Spliced *rps12* RNA in *ppr4* Mutants.

Top panel: Primer extension products were separated on a denaturing polyacrylamide gel. The radiolabeled primer and the extension products from spliced and unspliced RNAs are indicated. As a control, RNA transcribed in vitro from a spliced *rps12* cDNA was used as a template (cDNA). The two independent *ppr4* mutant samples have the genotype *ppr4-1/ppr4-2*. Bottom panel: Predicted products of poisoned primer extension reactions. Exon sequences are shaded in gray, and the primer sequence is underlined. Dideoxy CTP included in the extension reaction terminates reverse transcription at the first encountered G residue in the template, yielding 24- and 29-nucleotide (nt) extension products on spliced (S) and unspliced (U) RNA, respectively.

CRS2 and PPR4 are bound simultaneously to the intron (see Supplemental Figure 4 online; data not shown), but the results have been ambiguous. Because only a small fraction of the PPR4 (Figure 4) and CAF2/CRS2 (Ostheimer et al., 2003) in the stroma are bound to *rps12-int1*, the failure to detect strong coimmunoprecipitation does not eliminate the possibility that they can be found in the same complex. In any case, both the 5′ and 3′ intron segments were similarly enriched by immunoprecipitation with PPR4 (Figure 6), indicating that PPR4 either associates independently with both fragments and/or remains associated after the intron fragments bind one another.

Function of PPR4 in Ribosome Biogenesis

The defect in *rps12* splicing can account for the albino phenotype and plastid ribosome deficiency in *ppr4* mutants. *rps12* codes for ribosomal protein S12, found in the 30S ribosomal subunit. *Escherichia coli* S12 is essential for cell viability (http://www.shigen.nig.ac.jp/ecoli/pec/index.jsp). It interacts with the penultimate stem loop of the 16S rRNA (Cukras et al., 2003), positions the small and large subunits of the ribosome during translation elongation, and is involved in the maintenance of translational fidelity. Thus, the lack of mature *rps12* mRNA in *ppr4* mutants is expected to severely affect plastid ribosome function. This prediction is borne out by the global loss of chloroplast translation products and plastid rRNAs in *ppr4* mutants. Plants harboring the weak *ppr4-2* allele accumulate increased levels of pre-16S rRNA. We believe this to be a consequence of decreased *rps12* expression rather than a direct effect of reduced PPR4 function for the following reasons. First, 16S rRNA was not detectably enriched in the PPR4 RIP-chip assays, suggesting that PPR4 does not interact with pre-16S rRNA or with assembling 30S ribosomes. Furthermore, reduced S12 synthesis is predicted to lead to increased accumulation of pre-16S rRNA, based on studies of ribosome assembly and rRNA processing in *E. coli.* S12 is added to *E. coli* ribosomes late in the ribosome assembly pathway (Mizushima and Nomura, 1970; Culver and Noller, 1999), so reduced S12 synthesis is anticipated to result in the accumulation of late intermediates in 30S subunit assembly. Such assembly intermediates harbor incompletely processed rRNAs, as completed ribosome assembly is a prerequisite for the final rRNA processing steps in *E. coli* (Srivastava and Schlessinger, 1990). Results presented here support a model in which PPR4 is directly involved in S12 synthesis due to its role in *rps12 trans*-splicing, S12 is necessary for completed 30S subunit assembly, and completed 30S subunit maturation is necessary for the final processing steps of rRNA in chloroplasts, as in bacteria. Previously, we described another mutant, *hcf7*, with a 16S rRNA processing defect similar to that observed in weak *ppr4* mutants (Barkan, 1993). The *hcf7* gene product has not been identified, although the results of complementation tests indicate that *hcf7* and *ppr4* are not allelic (data not shown). In light of the findings presented here, it seems possible that HCF7 is necessary for the expression of a late assembling protein of the small ribosomal subunit in chloroplasts.

T-DNA insertions in the *Arabidopsis ppr4* ortholog cause an embryo-lethal phenotype (see Results), as do insertions in the *Arabidopsis* ortholog of maize *ppr2* (At3g06430; see EMB2750 at http://www.seedgenes.org). By contrast, exonic insertions in maize *ppr2* and *ppr4* condition albino seedlings that lack plastid ribosomes (Williams and Barkan, 2003; this article). In fact, embryo lethality is commonly observed for mutations in *Arabidopsis* genes encoding chloroplast-targeted PPR proteins (Tzafrir et al., 2004; Cushing et al., 2005). We suspect that embryo lethality in many of these cases is the result of a severe defect in the plastid translation machinery. Strong plastid translation defects seem to impact maize and *Arabidopsis* very differently, as mutations in maize that condition albino seedlings with severe plastid ribosome deficiencies are commonly observed (e.g., *ppr2*, *ppr4*, *crs2*, *iojap*, *caf1*, and *caf2*) (Walbot and Coe, 1979; Jenkins et al., 1997; Ostheimer et al., 2003; Williams and Barkan, 2003), but analogous *Arabidopsis* mutants have not been reported. Furthermore, in *Arabidopsis*, embryo lethality would be anticipated to result from the absence of plastid translation because the *Arabidopsis* chloroplast genome harbors three open reading frames, *accD*, *ycf1*, and *ycf2*, that are essential for cellular viability (Drescher et al., 2000; Kode et al., 2005). These open reading frames are lacking in the maize chloroplast genome (Maier et al., 1995), and this difference in plastid gene content may account for the seedling viability of maize mutants lacking plastid ribosomes. Therefore, maize is a particularly useful organism in which to study nuclear genes like *ppr4*, *crs2*, *caf1*, and *caf2* that are required for the expression of plastid genes encoding components of the translation machinery.

RIP-Chip as a Tool for Facilitating the Genetic Analysis of Chloroplast Gene Expression

RIP-chip data complement genetic analysis of RNA binding proteins by helping to distinguish direct from indirect effects of a mutation. RIP-chip data are also useful to guide analysis of a mutant when the phenotype is uninformative due to genetic redundancy or pleiotropy. For example, identification of specific plastid gene expression defects that underlie a nonphotosynthetic mutant phenotype can be straightforward when a subset of chloroplast-encoded proteins (e.g., a single enzyme complex) accumulate to reduced levels. In such instances, systematic analysis of the expression of genes encoding the missing proteins can identify RNA metabolism or translation defects responsible for the protein losses. However, for mutations like those in *ppr4*, the global protein deficiencies are not very informative, as they suggest a defect in the expression of one or more of the large number of nuclear and plastid genes that contribute to basal chloroplast gene expression (tRNAs, ribosomal proteins, etc.). It is labor intensive to assess the expression of each candidate gene in search of the underlying molecular lesion. This problem is exacerbated in albino mutants lacking plastid ribosomes because they exhibit stereotypical defects in chloroplast RNA metabolism (Han et al., 1992, 1995; Hess et al., 1993; Jenkins et al., 1997; Williams and Barkan, 2003). These aberrant transcript patterns are caused in part by the loss of the plastid-encoded RNA polymerase, as the nuclear-encoded polymerase activity recognizes a distinct set of promoters (Hajdukiewicz et al., 1997).

Because of these factors, RIP-chip data are particularly valuable for guiding the phenotypic analysis of mutations that cause a global defect in chloroplast translation. RIP-chip data focus attention on a small set of candidate substrate RNAs, obviating the need to examine in detail the expression of all of the many chloroplast genes that contribute to the gene expression machinery. In the analysis of *ppr4* functions, the defect in *rps12* mRNA metabolism may ultimately have been discovered in *ppr4* mutants without the use of RIP-chip, but the RIP-chip data led much more quickly to the discovery of this defect. Thus, the combined use of RIP-chip and genetic analysis in maize is expected to enhance progress in understanding the functions of the large set of nuclear genes in plants that function in the expression of components of the plastid translation apparatus.

METHODS

Nucleotide Sequence Analysis of *ppr4*

The nucleotide sequence of the rice (*Oryza sativa*) gene Os04g58780 was used to query the maize (*Zea mays*) sequence at the PlantGDB database (http://www.plantgdb.org/PlantGDB-cgi/blast/PlantGDBblast). The single maize contig identified exhibits high identity to the rice sequence at the amino acid level (83%), had the same intron/exon structure, and detected the rice gene as its top hit when used to query the rice genome. A *ppr4* cDNA was obtained from the University of Arizona's collection (accession number DR967823.1), and its nucleotide sequence was determined. The cDNA sequence is deposited in GenBank under accession number DQ508419.

Plant Material

The two *ppr4* mutant alleles were identified in a reverse-genetic screen of a collection of ~2300 *Mu*-induced nonphotosynthetic maize mutants (http://chloroplast.uoregon.edu/). The PCR-based screen was performed with a *ppr4*-specific primer (5′-ACTCTAGCCCAACCTTTAACGTGGTA-3′) in conjunction with a *Mu* terminal inverted repeat primer (5′-AGAGAA-GCCAACGCCAWCGCCTCYATTTCGTC-3′) using a method analogous to that described previously for *ppr2* (Williams and Barkan, 2003). Allelism between *ppr4-1* and *ppr4-2* was tested by intercrossing the phenotypically wild-type siblings of mutant plants (which include both +/+ and +/− genotypes). Altogether, 101 independent crosses were performed, 40 of which yielded ~25% pale green seedlings. These numbers fit the expectation for Mendelian segregation of single, allelic recessive mutations in the two lines that cause a chlorophyll deficiency. The phenotype of the mutant noncomplementing progeny was intermediate between that conditioned by the two parental alleles. Taken together, these results confirmed that the mutant phenotypes segregating in the *ppr4-1* and *ppr4-2* lines are due to the *Mu* insertions in *ppr4.*

Maize *hcf7* mutants were used as controls in this work: *hcf7* mutants are pale green and show reduced polysome assembly and aberrant metabolism of 16S rRNA (Barkan, 1993). The inbred line B73 (Pioneer HiBred) was used as the source of wild-type tissue for RIP-chip and chloroplast fractionation experiments. Seedlings were grown in soil in a growth chamber under a 16-h-light/8-h-dark cycle at 26°C and harvested between 7 and 10 d after planting.

Nucleic Acid Extraction and Analysis

Seedling leaf DNA for PCR amplification was isolated using plant DNAzol reagent (Invitrogen) according to the manufacturer's protocol. Leaf RNA was isolated using Tri reagent (Molecular Research Center). RNA gel blot hybridizations were performed as described previously with 5 μg of total leaf RNA (Barkan et al., 1994). Hybridization was performed at 65°C in Church hybridization buffer (Sambrook et al., 1989); blots were washed at 65°C in 0.2× SSC and 0.2% SDS. The following DNA fragments were used as probes for chloroplast RNAs: rps12 exon 1, 69281 to 69460; rps12 intron 1 5′, 68793 to 69302; rps12 intron 1 3′, 93161 to 93570; rps12 exon 2, 92876 to 93078; residue numbers from GenBank accession number X86563; rrn16 and rrn23, Bam13 fragment and 3-kb *Pst*I fragment of chloroplast DNA, respectively, described by Barkan (1993).

For poisoned primer extension experiments, 20 pmol of an *rps12-exon2* oligonucleotide (5′-GGTTTTTTGGGGTTGATAG-3′) (Figure 8) or *rps12-exon3* oligonucleotide (5′-TTGGCTTTTTGGCCCCATATT-3′) (see Supplemental Figure 3B online) was radiolabeled at its 5′ end by incubation with [γ-32P]ATP and T4 polynucleotide kinase (New England Biolabs). Four micrograms of leaf RNA was heated to 95°C and annealed to the oligonucleotide by slow cooling to 45°C in 50 mM Tris-HCl, pH 8.5, 500 mM KCl, and 0.5 mM each of dATP, dGTP, dTTP, and ddCTP (10-μL reaction volume). Primer extension was initiated by adding 30 units of AMV reverse transcriptase (Promega), and the reactions were incubated at 45°C for 30 min. The reactions were stopped by adding 12 μL of 80% formamide and 0.25× TBE (1× TBE is 90 mM Tris-Borate, pH 8.3, and 2 mM EDTA). Ten microliters of each sample was applied to a 12% polyacrylamide gel containing 8 M urea and electrophoresed in 1× TBE. The gel was exposed to a PhosphorImager screen (Molecular Dynamics) and analyzed using ImageQuant software (GE Healthcare).

For RT-PCR analysis of *ppr4* mRNA levels in mutant plants, primers were designed that spanned an intron, such that the amplification products from mRNA and genomic DNA could be distinguished. cDNA was generated from the indicated amounts of total leaf RNA by priming reverse transcription with the gene-specific primers PPR4 794REV (5′-CCTCGCTTGGCATAATACAC-3′) or α-tubulin REV (5′-AACACCAA-GAATCCCTGCAGCCCAGTGC-3′). Primer was annealed to RNA in a

10-μL reaction containing 2 μL RNA and 1 μL of a 50 μM primer stock in annealing buffer (150 mM NaCl and 20 mM Tris-HCl, pH 8.5) by heating to 95°C for 30 s and cooling at 4°C for 2 min. This mixture was added to 10 μL of 2× Promega AMV buffer (100 mM Tris-HCl, pH 8.3, 100 mM KCl, 20 mM $MgCl_2$, 1 mM spermidine, and 20 mM DTT) supplemented with 2 mM deoxynucleotide triphosphate and 30 units of RNAsin (Promega). Primer extension was performed with 5 units of AMV reverse transcriptase (Promega) at 48°C for 1 h. PCR amplification was performed with the reverse primers described above, in conjunction with the forward primers PPR4 591FOR (5′-GCGGGCGCGCTGGGTCGAA-3′) or α-tubulin FOR (5′-AGCCCGATGGCACCATGCCCAGTGATACCT-3′). PCR reactions (30 μL) contained 2 μL of cDNA, 1 μM of each primer in 1× PCR buffer (Ex Taq buffer; TaKaRa), 0.8 mM deoxynucleotide triphosphate, 10% DMSO, and 1.25 units of Ex-Taq (TaKaRa) and were amplified under the following conditions: PPR4, 94°C/2 min, followed by 34 cycles of 94°C/30 s, 52°C/30 s, 72°C/30 s, and a final extension of 72°C/5 min; tubulin, 94°C/2 min, followed by 30 cycles of 94°C/30 s, 58°C/30 s, 72°C/30 s, and a final extension of 72°C/5 min. Ten microliters of each reaction were electrophoresed in 1.5% agarose gels. The tubulin cDNA was visualized by staining the gel with ethidium bromide. The *ppr4* cDNA was visualized by DNA gel blotting, using a probe generated from a *ppr4* cDNA clone using the same primers used for RT-PCR.

Antibody Production

Recombinant PPR4 was generated by expressing amino acids 615 to 886 in the vector pet28b (Novagen) to generate a fusion protein with a C-terminal 6xhistidine tag. This tagged PPR4 fragment was purified on a Ni-NTA agarose column (Qiagen) and used to generate polyclonal antisera in rabbits. The same PPR4 fragment was used to affinity purify the antisera prior to their use for RIP-chip and immunoblotting experiments.

Chloroplast Fractionation and Protein Analyses

Total leaf protein was extracted and analyzed by immunoblotting as described previously (Barkan, 1998). Antisera to OEC23, AtpA, D1, PsaD, and PetD are described by Voelker and Barkan (1995) and McCormac and Barkan (1999). Chloroplast subfractions were those described by Williams and Barkan (2003). Stromal extracts (0.5 mg of stromal protein per experiment) were fractionated by sedimentation through sucrose gradients according to Jenkins and Barkan (2001).

RIP-Chip and Slot Blot Hybridization Analysis of RNAs Bound to PPR4

The maize chloroplast microarray and RIP-chip procedure are described by Schmitz-Linneweber et al. (2005). Briefly, 2 μL of affinity-purified anti-PPR4 antibody was incubated with 100 μL of stromal extract (~500 μg stromal protein) from the inbred line B73 or from *ppr4-1/ppr4-2* mutant (~100 μg stromal protein). The antibody was collected by incubation with formaldehyde-fixed StaphA cells (IG sorb; Enzyme Centre). RNA was isolated from pellet and supernatant fractions by phenol-chloroform extraction and labeled with Cy3 and Cy5 using the Micromax ASAP RNA labeling kit (Perkin-Elmer Life Sciences). Labeled RNA was purified using Qiaquick spin columns (Qiagen) and hybridized to microarrays covering the entire chloroplast chromosome in overlapping DNA fragments (Array Express accession number A-MEXP-164). Slides were scanned with a Genepix 4000B microarray scanner (Axon Instruments). Data were filtered against elements with low signal-to-noise ratios, and local background was calculated according to default parameters in Genepix Pro 6.0 software. Only spots with a signal-to-background ratio >4 and for which 60% of pixels have a F532 fluorescent signal >2 SD above background were chosen for further analysis. Fragments for which fewer than two spots per array passed these cutoffs were not used for subsequent analyses and appear as gaps when enrichment ratios are plotted according to chromosomal position. Background-subtracted data were used to calculate the median of ratios (pellet RNA F635: supernatant RNA F532). After $\log_2$ transformation, this value is called the enrichment ratio. Normalization was done according to the median $\log_2$F635/F532 value for all above background spots on each array.

RNAs for slot blot hybridizations were prepared in the same way as those used for RIP-chip assays. However, instead of using them to probe an array, they were applied to a nylon membrane with a slot blot manifold and hybridized to specific radiolabeled PCR fragments. The PCR fragments were body-labeled with [^{32}P]dCTP by the random priming method. Hybridization and washing were performed as described for the slot blot analyses by Schmitz-Linneweber et al. (2005). One-sixth of the RNA recovered from each immunoprecipitation supernatant and one-third of the RNA recovered from each immunoprecipitation pellet were applied to each slot.

Accession Numbers

Sequence data for *ppr4* cDNA can be found in the GenBank data library under accession number DQ508419. The PPR4 RIP-chip data have been deposited at MIAME-Express under accession number E-MEXP-716.

Supplemental Data

The following materials are available in the online version of this article.

Supplemental Figure 1. Positions of T-DNA Insertions in At PPR4 (At5g04810).

Supplemental Figure 2. Median Log_2-Transformed Enrichment Ratios for Eeplicate Spots in Each of the Four PPR4 RIP-Chip Experiments Plotted against Fragment Number.

Supplemental Figure 3. Analysis of Transcripts from Putative Secondary Targets of PPR4 in *ppr4* Mutants.

Supplemental Figure 4. Assay for Coimmunoprecipitation of PPR4 with CAF2/CRS2 Complex.

Supplemental Table 1. Median Log_2 Ratios, Number of Spots Above Background for Each PCR Product on the Array, and SD Values for All Four RIP-Chip Experiments.

Supplemental Table 2. Values for Combined Replicate RIP-Chip Data Sets.

ACKNOWLEDGMENTS

We thank Kenny Watkins for useful discussions. This work was supported by a postdoctoral fellowship to C.S.-L. from the Deutsche Forschungsgemeinschaft and by grants to A.B. from the National Science Foundation (MCB-0314597 and DBI-0421799).

Received July 26, 2006; revised August 23, 2006; accepted September 18, 2006; published October 13, 2006.

REFERENCES

Alonso, J.M., et al. (2003). Genome-wide insertional mutagenesis of *Arabidopsis thaliana.* Science **301,** 653–657.

Auchincloss, A., Zerges, W., Perron, K., Girard-Bascou, J., and Rochaix, J.-D. (2002). Characterization of Tbc2, a nucleus-encoded factor specifically required for translation of the chloroplast *psbC* mRNA in *Chlamydomonas reinhardtii.* J. Cell Biol. **157,** 953–962.

Barkan, A. (1993). Nuclear mutants of maize with defects in chloroplast polysome assembly have altered chloroplast RNA metabolism. Plant Cell **5,** 389–402.

Barkan, A. (1998). Approaches to investigating nuclear genes that function in chloroplast biogenesis in land plants. Methods Enzymol. **297,** 38–57.

Barkan, A. (2004). Intron splicing in plant organelles. In Molecular Biology and Biotechnology of Plant Organelles, H. Daniell and C. Chase, eds (Dordrecht, The Netherlands: Springer), pp. 295–322.

Barkan, A., Walker, M., Nolasco, M., and Johnson, D. (1994). A nuclear mutation in maize blocks the processing and translation of several chloroplast mRNAs and provides evidence for the differential translation of alternative mRNA forms. EMBO J. **13,** 3170–3181.

Bentolila, S., Alfonso, A.A., and Hanson, M.R. (2002). A pentatricopeptide repeat-containing gene restores fertility to cytoplasmic male-sterile plants. Proc. Natl. Acad. Sci. USA **99,** 10887–10892.

Carignani, G., Groudinsky, O., Frezza, D., Schiavon, E., Bergantino, E., and Slonimski, P.P. (1983). An mRNA maturase is encoded by the first intron of the mitochondrial gene for the subunit I of cytochrome oxidase in *S. cerevisiae.* Cell **35,** 733–742.

Carignani, G., Netter, P., Bergantino, E., and Robineau, S. (1986). Expression of the mitochondrial split gene coding for cytochrome oxidase subunit I in *S. cerevisiae*: RNA splicing pathway. Curr. Genet. **11,** 55–63.

Coffin, J.W., Dhillon, R., Ritzel, R.G., and Nargang, F.E. (1997). The *Neurospora crassa cya-5* nuclear gene encodes a protein with a region of homology to the *Saccharomyces cerevisiae* PET309 protein and is required in a post-transcriptional step for the expression of the mitochondrially encoded COXI protein. Curr. Genet. **32,** 273–280.

Cukras, A.R., Southworth, D.R., Brunelle, J.L., Culver, G.M., and Green, R. (2003). Ribosomal proteins S12 and S13 function as control elements for translocation of the mRNA:tRNA complex. Mol. Cell **12,** 321–328.

Culver, G.M., and Noller, H.F. (1999). Efficient reconstitution of functional *Escherichia coli* 30S ribosomal subunits from a complete set of recombinant small subunit ribosomal proteins. RNA **5,** 832–843.

Cushing, D.A., Forsthoefel, N.R., Gestaut, D.R., and Vernon, D.M. (2005). *Arabidopsis* emb175 and other ppr knockout mutants reveal essential roles for pentatricopeptide repeat (PPR) proteins in plant embryogenesis. Planta **221,** 424–436.

Dahlberg, A.E., Dahlberg, J.E., Lund, E., Tokimatsu, H., Rabson, A.B., Calvert, P.C., Reynolds, F., and Zahalak, M. (1978). Processing of the 5′ end of *Escherichia coli* 16S ribosomal RNA. Proc. Natl. Acad. Sci. USA **75,** 3598–3602.

Desloire, S., et al. (2003). Identification of the fertility restoration locus, Rfo, in radish, as a member of the pentatricopeptide-repeat protein family. EMBO Rep. **4,** 588–594.

Ding, Y.H., Liu, N.Y., Tang, Z.S., Liu, J., and Yang, W.C. (2006). *Arabidopsis* GLUTAMINE-RICH PROTEIN23 is essential for early embryogenesis and encodes a novel nuclear PPR motif protein that interacts with RNA polymerase II subunit III. Plant Cell **18,** 815–830.

Drescher, A., Ruf, S., Calsa, T., Jr., Carrer, H., and Bock, R. (2000). The two largest chloroplast genome-encoded open reading frames of higher plants are essential genes. Plant J. **22,** 97–104.

Dyall, S.D., Brown, M.T., and Johnson, P.J. (2004). Ancient invasions: From endosymbionts to organelles. Science **304,** 253–257.

Emanuelsson, O., Nielsen, H., Brunak, S., and von Heijne, G. (2000). Predicting subcellular localization of proteins based on their N-terminal amino acid sequence. J. Mol. Biol. **300,** 1005–1016.

Fisk, D.G., Walker, M.B., and Barkan, A. (1999). Molecular cloning of the maize gene *crp1* reveals similarity between regulators of mitochondrial and chloroplast gene expression. EMBO J. **18,** 2621–2630.

Goldschmidt-Clermont, M., Girard-Bascou, J., Choquet, Y., and Rochaix, J.D. (1990). Trans-splicing mutants of *Chlamydomonas reinhardtii.* Mol. Gen. Genet. **223,** 417–425.

Gray, M.W. (2004). The evolutionary origins of plant organelles. In Molecular Biology and Biotechnology of Plant Organelles, Chloroplasts and Mitochondria, H. Daniell and C. Chase, eds (Dordrecht, The Netherlands: Springer), pp. 15–36.

Hajdukiewicz, P.T., Allison, L.A., and Maliga, P. (1997). The two RNA polymerases encoded by the nuclear and the plastid compartments transcribe distinct groups of genes in tobacco plastids. EMBO J. **16,** 4041–4048.

Han, C.D., Coe, E.H., Jr., and Martienssen, R.A. (1992). Molecular cloning and characterization of iojap (ij), a pattern striping gene of maize. EMBO J. **11,** 4037–4046.

Han, C.-d., Derby, R.J., Schnable, P.S., and Martienssen, R.A. (1995). Characterization of the plastids affected by class II albino mutations of maize at the morphological and transcript levels. Maydica **40,** 13–22.

Han, C.-D., Patrie, W., Polacco, M., and Coe, E.H. (1993). Aberrations in plastid transcripts and deficiency of plastid DNA in striped and albino mutants in maize. Planta **191,** 552–563.

Hashimoto, M., Endo, T., Peltier, G., Tasaka, M., and Shikanai, T. (2003). A nucleus-encoded factor, CRR2, is essential for the expression of chloroplast ndhB in *Arabidopsis.* Plant J. **36,** 541–549.

Hess, W.R., Prombona, A., Fieder, B., Subramanian, A.R., and Borner, T. (1993). Chloroplast *rps15* and the *rpoB/C1/C2* gene cluster are strongly transcribed in ribosome-deficient plastids: Evidence for a functioning non-chloroplast-encoded RNA polymerase. EMBO J. **12,** 563–571.

Hildebrand, M., Hallick, R.B., Passavant, C.W., and Bourque, D.P. (1988). Trans-splicing in chloroplasts: The rps 12 loci of *Nicotiana tabacum.* Proc. Natl. Acad. Sci. USA **85,** 372–376.

Huang, H.R., Rowe, C.E., Mohr, S., Jiang, Y., Lambowitz, A.M., and Perlman, P.S. (2005). The splicing of yeast mitochondrial group I and group II introns requires a DEAD-box protein with RNA chaperone function. Proc. Natl. Acad. Sci. USA **102,** 163–168.

Ikeda, T.M., and Gray, M.W. (1999). Characterization of a DNA-binding protein implicated in transcription in wheat mitochondria. Mol. Cell. Biol. **19,** 8113–8122.

Jenkins, B.D., and Barkan, A. (2001). Recruitment of a peptidyl-tRNA hydrolase as a facilitator of group II intron splicing in chloroplasts. EMBO J. **20,** 872–879.

Jenkins, B.D., Kulhanek, D.J., and Barkan, A. (1997). Nuclear mutations that block group II RNA splicing in maize chloroplasts reveal several intron classes with distinct requirements for splicing factors. Plant Cell **9,** 283–296.

Kazama, T., and Toriyama, K. (2003). A pentatricopeptide repeat-containing gene that promotes the processing of aberrant atp6 RNA of cytoplasmic male-sterile rice. FEBS Lett. **544,** 99–102.

Kode, V., Mudd, E.A., Iamtham, S., and Day, A. (2005). The tobacco plastid accD gene is essential and is required for leaf development. Plant J. **44,** 237–244.

Koizuka, N., Imai, R., Fujimoto, H., Hayakawa, T., Kimura, Y., Kohno-Murase, J., Sakai, T., Kawasaki, S., and Imamura, J. (2003). Genetic characterization of a pentatricopeptide repeat protein gene, orf687, that restores fertility in the cytoplasmic male-sterile Kosena radish. Plant J. **34,** 407–415.

Koller, B., Fromm, H., Galun, E., and Edelman, M. (1987). Evidence for in vivo trans splicing of pre-mRNAs in tobacco chloroplasts. Cell **48,** 111–119.

Kotera, E., Tasaka, M., and Shikanai, T. (2005). A pentatricopeptide repeat protein is essential for RNA editing in chloroplasts. Nature **433,** 326–330.

Lahmy, S., Barneche, F., Derancourt, J., Filipowicz, W., Delseny, M., and Echeverria, M. (2000). A chloroplastic RNA-binding protein is a new member of the PPR family. FEBS Lett. **480,** 255–260.

Lambowitz, A.M., and Perlman, P.S. (1990). Involvement of aminoacyl-tRNA synthetases and other proteins in group I and group II intron splicing. Trends Biochem. Sci. **15,** 440–444.

Lown, F., Watson, A., and Purton, S. (2001). *Chlamydomonas* nuclear mutants that fail to assemble respiratory or photosynthetic electron transfer complexes. Biochem. Soc. Trans. **29,** 452–455.

Lurin, C., et al. (2004). Genome-wide analysis of *Arabidopsis* pentatricopeptide repeat proteins reveals their essential role in organelle biogenesis. Plant Cell **16,** 2089–2103.

Maier, R.M., Neckermann, K., Igloi, G.L., and Kossel, H. (1995). Complete sequence of the maize chloroplast genome: Gene content, hotspots of divergence and fine tuning of genetic information by transcript editing. J. Mol. Biol. **251,** 614–628.

Mancebo, R., Zhou, X., Shillinglaw, W., Henzel, W., and Macdonald, P. (2001). BSF binds specifically to the *bicoid* mRNA 3′ untranslated region and contributes to stabilization of *bicoid* mRNA. Mol. Cell. Biol. **21,** 3462–3471.

Manthey, G.M., and McEwen, J.E. (1995). The product of the nuclear gene *PET309* is required for translation of mature mRNA and stability or production of intron-containing RNAs derived from the mitochondrial *COX1* locus of *Saccharomyces cerevisiae.* EMBO J. **14,** 4031–4043.

McCormac, D.J., and Barkan, A. (1999). A nuclear gene in maize required for the translation of the chloroplast *atpB/E* mRNA. Plant Cell **11,** 1709–1716.

Meierhoff, K., Felder, S., Nakamura, T., Bechtold, N., and Schuster, G. (2003). HCF152, an *Arabidopsis* RNA binding pentatricopeptide repeat protein involved in the processing of chloroplast *psbB-psbT-psbH-petB-petD* RNAs. Plant Cell **15,** 1480–1495.

Merendino, L., Perron, K., Rahire, M., Howald, I., Rochaix, J.D., and Goldschmidt-Clermont, M. (2006). A novel multifunctional factor involved in trans-splicing of chloroplast introns in Chlamydomonas. Nucleic Acids Res. **34,** 262–274.

Michel, F., and Ferat, J.L. (1995). Structure and activities of group II introns. Annu. Rev. Biochem. **64,** 435–461.

Michel, F., Umesono, K., and Ozeki, H. (1989). Comparative and functional anatomy of group II catalytic introns–A review. Gene **82,** 5–30.

Mili, S., and Pinol-Roma, S. (2003). LRP130, a pentatricopeptide motif protein with a noncanonical RNA-binding domain, is bound in vivo to mitochondrial and nuclear RNAs. Mol. Cell. Biol. **23,** 4972–4982.

Mingler, M.K., Hingst, A.M., Clement, S.L., Yu, L.E., Reifur, L., and Koslowsky, D.J. (2006). Identification of pentatricopeptide repeat proteins in *Trypanosoma brucei.* Mol. Biochem. Parasitol. **150,** 37–45.

Mizushima, S., and Nomura, M. (1970). Assembly mapping of 30S ribosomal proteins from E. coli. Nature **226,** 1214.

Mohr, S., Matsuura, M., Perlman, P.S., and Lambowitz, A.M. (2006). A DEAD-box protein alone promotes group II intron splicing and reverse splicing by acting as an RNA chaperone. Proc. Natl. Acad. Sci. USA **103,** 3569–3574.

Nakamura, T., Meierhoff, K., Westhoff, P., and Schuster, G. (2003). RNA-binding properties of HCF152, an *Arabidopsis* PPR protein involved in the processing of chloroplast RNA. Eur. J. Biochem. **270,** 4070–4081.

Ostheimer, G.J., Williams-Carrier, R., Belcher, S., Osborne, E., Gierke, J., and Barkan, A. (2003). Group II intron splicing factors derived by diversification of an ancient RNA-binding domain. EMBO J. **22,** 3919–3929.

Perron, K., Goldschmidt-Clermont, M., and Rochaix, J.D. (1999). A factor related to pseudouridine synthases is required for chloroplast group II intron trans-splicing in *Chlamydomonas reinhardtii.* EMBO J. **18,** 6481–6490.

Prasad, A.M., Sivanandan, C., Resminath, R., Thakare, D.R., Bhat, S.R., and Srinivasan. (2005). Cloning and characterization of a pentatricopeptide protein encoding gene (LOJ) that is specifically expressed in lateral organ junctions in *Arabidopsis thaliana.* Gene **353,** 67–79.

Rivier, C., Goldschmidt-Clermont, M., and Rochaix, J.D. (2001). Identification of an RNA-protein complex involved in chloroplast group II intron trans-splicing in *Chlamydomonas reinhardtii.* EMBO J. **20,** 1765–1773.

Sambrook, J., Fritsch, E.F., and Maniatis, T. (1989). Molecular Cloning: A Laboratory Manual. (Cold Spring Harbor, NY: Cold Spring Harbor Laboratory Press).

Schmitz-Linneweber, C., Williams-Carrier, R., and Barkan, A. (2005). RNA immunoprecipitation and microarray analysis show a chloroplast pentatricopeptide repeat protein to be associated with the 5′ region of mRNAs whose translation it activates. Plant Cell **17,** 2791–2804.

Small, I., and Peeters, N. (2000). The PPR motif - A TPR-related motif prevalent in plant organellar proteins. Trends Biochem. Sci. **25,** 46–47.

Small, I., Peeters, N., Legeai, F., and Lurin, C. (2004). Predotar: A tool for rapidly screening proteomes for N-terminal targeting sequences. Proteomics **4,** 1581–1590.

Srivastava, A., and Schlessinger, D. (1989). Processing pathway of *E. coli* 16S precursor rRNA. Nucleic Acids Res. **17,** 1649–1663.

Srivastava, A.K., and Schlessinger, D. (1990). Mechanism and regulation of bacterial ribosomal RNA processing. Annu. Rev. Microbiol. **44,** 105–129.

Stern, D.B., Hanson, M.R., and Barkan, A. (2004). Genetics and genomics of chloroplast biogenesis: Maize as a model system. Trends Plant Sci. **9,** 293–301.

Till, B., Schmitz-Linneweber, C., Williams-Carrier, R., and Barkan, A. (2001). CRS1 is a novel group II intron splicing factor that was derived from a domain of ancient origin. RNA **7,** 1227–1238.

Turmel, M., Otis, C., and Lemieux, C. (2002). The chloroplast and mitochondrial genome sequences of the charophyte *Chaetosphaeridium globosum*: Insights into the timing of the events that restructured organelle DNAs within the green algal lineage that led to land plants. Proc. Natl. Acad. Sci. USA **99,** 11275–11280.

Turmel, M., Otis, C., and Lemieux, C. (2005). The complete chloroplast DNA sequences of the charophycean green algae Staurastrum and Zygnema reveal that the chloroplast genome underwent extensive changes during the evolution of the Zygnematales. BMC Biol **3,** 22.

Tzafrir, I., Pena-Muralla, R., Dickerman, A., Berg, M., Rogers, R., Hutchens, S., Sweeney, T.C., McElver, J., Aux, G., Patton, D., and Meinke, D. (2004). Identification of genes required for embryo development in *Arabidopsis.* Plant Physiol. **135,** 1206–1220.

Voelker, R., and Barkan, A. (1995). Two nuclear mutations disrupt distinct pathways for targeting proteins to the chloroplast thylakoid. EMBO J. **14,** 3905–3914.

Walbot, V., and Coe, E.H. (1979). Nuclear gene *iojap* conditions a programmed change to ribosome-less plastids in *Zea mays.* Proc. Natl. Acad. Sci. USA **76,** 2760–2764.

Wang, Z., et al. (2006). Cytoplasmic male sterility of rice with boro II cytoplasm is caused by a cytotoxic peptide and is restored by two related PPR motif genes via distinct modes of mRNA silencing. Plant Cell **18,** 676–687.

Williams, P.M., and Barkan, A. (2003). A chloroplast-localized PPR protein required for plastid ribosome accumulation. Plant J. **36,** 675–686.

Xu, F., Morin, C., Mitchell, G., Ackerley, C., and Robinson, B.H. (2004). The role of the LRPPRC (leucine-rich pentatricopeptide repeat cassette) gene in cytochrome oxidase assembly: Mutation causes lowered levels of COX (cytochrome c oxidase) I and COX III mRNA. Biochem. J. **382,** 331–336.

Yamazaki, H., Tasaka, M., and Shikanai, T. (2004). PPR motifs of the nucleus-encoded factor, PGR3, function in the selective and distinct steps of chloroplast gene expression in *Arabidopsis.* Plant J. **38,** 152–163.